AFRL-AFOSR-VA-TR-2016-0053

Reconfigurable Optical Directed-Logic Circuits

Jacob Robinson
WILLIAM MARSH RICE UNIV HOUSTON TX

11/20/2015
Final Report

Air Force Research Laboratory
AF Office Of Scientific Research (AFOSR)/ RTA1
Arlington, Virginia 22203
Air Force Materiel Command

REPORT DOCUMENTATION PAGE

Form Approved
OMB No. 0704-0188

PLEASE DO NOT RETURN YOUR FORM TO THE ABOVE ORGANIZATION.

1. REPORT DATE *(DD-MM-YYYY)*	2. REPORT TYPE	3. DATES COVERED *(From - To)*
10-11-2015	Final	2 Jan 2012-14 June 2015

4. TITLE AND SUBTITLE

Reconfigurable Optical Directed-Logic Circuits

5a. CONTRACT NUMBER

FA9550-12-1-0261

5b. GRANT NUMBER

FA9550-12-1-0261

5c. PROGRAM ELEMENT NUMBER

6. AUTHOR(S)

Robinson, Jacob

5d. PROJECT NUMBER

5e. TASK NUMBER

5f. WORK UNIT NUMBER

7. PERFORMING ORGANIZATION NAME(S) AND ADDRESS(ES)

Rice University
6100 Main Street
Houston, TX 70005

8. PERFORMING ORGANIZATION REPORT NUMBER

9. SPONSORING/MONITORING AGENCY NAME(S) AND ADDRESS(ES)

Air Force Office of Scientific Research
875 North Randolph Street
Arlington, VA 22203

10. SPONSOR/MONITOR'S ACRONYM(S)

11. SPONSOR/MONITOR'S REPORT NUMBER(S)

12. DISTRIBUTION/AVAILABILITY STATEMENT

Approved for Public Release; Distribution is Unlimited

13. SUPPLEMENTARY NOTES

14. ABSTRACT

Directed logic (DL) is an innovative logic paradigm that minimizes the latency in calculating a complicated logic function by taking advantage of the fast and low-loss propagation of light. DL can enhance the performance of digital systems for real-time applications that are especially important for Air Force missions, such as video analysis, object recognition, visualization and battle management. DL can also provide very fast network routing functions, which enable highly efficient packet-switched interconnection networks for high-performance computing.
A DL circuit is formed by a network of optical switches controlled by the input logic signals. The optical wave travelling in the switch network calculates a logic function of the control signals. While it takes time for each switch to respond to a change in its control signal, all the switches operate simultaneously, and their switching delays do not accumulate. This is in contrast to conventional logic circuits where gate delays are cascaded, resulting in a large latency in a complex logic circuit.

15. SUBJECT TERMS

directed logic, optical, circuits

16. SECURITY CLASSIFICATION OF:			17. LIMITATION OF ABSTRACT	18. NUMBER OF PAGES	19a. NAME OF RESPONSIBLE PERSON
a. REPORT	b. ABSTRACT	c. THIS PAGE			AFSOR
U	U	U	UU	11	19b. TELEPHONE NUMBER *(Include area code)*

Standard Form 298 (Rev. 8/98)
Prescribed by ANSI Std. Z39.18

INSTRUCTIONS FOR COMPLETING SF 298

1. REPORT DATE. Full publication date, including day, month, if available. Must cite at least the year and be Year 2000 compliant, e.g. 30-06-1998; xx-06-1998; xx-xx-1998.

2. REPORT TYPE. State the type of report, such as final, technical, interim, memorandum, master's thesis, progress, quarterly, research, special, group study, etc.

3. DATES COVERED. Indicate the time during which the work was performed and the report was written, e.g., Jun 1997 - Jun 1998; 1-10 Jun 1996; May - Nov 1998; Nov 1998.

4. TITLE. Enter title and subtitle with volume number and part number, if applicable. On classified documents, enter the title classification in parentheses.

5a. CONTRACT NUMBER. Enter all contract numbers as they appear in the report, e.g. F33615-86-C-5169.

5b. GRANT NUMBER. Enter all grant numbers as they appear in the report, e.g. AFOSR-82-1234.

5c. PROGRAM ELEMENT NUMBER. Enter all program element numbers as they appear in the report, e.g. 61101A.

5d. PROJECT NUMBER. Enter all project numbers as they appear in the report, e.g. 1F665702D1257; ILIR.

5e. TASK NUMBER. Enter all task numbers as they appear in the report, e.g. 05; RF0330201; T4112.

5f. WORK UNIT NUMBER. Enter all work unit numbers as they appear in the report, e.g. 001; AFAPL30480105.

6. AUTHOR(S). Enter name(s) of person(s) responsible for writing the report, performing the research, or credited with the content of the report. The form of entry is the last name, first name, middle initial, and additional qualifiers separated by commas, e.g. Smith, Richard, J, Jr.

7. PERFORMING ORGANIZATION NAME(S) AND ADDRESS(ES). Self-explanatory.

8. PERFORMING ORGANIZATION REPORT NUMBER. Enter all unique alphanumeric report numbers assigned by the performing organization, e.g. BRL-1234; AFWL-TR-85-4017-Vol-21-PT-2.

9. SPONSORING/MONITORING AGENCY NAME(S) AND ADDRESS(ES). Enter the name and address of the organization(s) financially responsible for and monitoring the work.

10. SPONSOR/MONITOR'S ACRONYM(S). Enter, if available, e.g. BRL, ARDEC, NADC.

11. SPONSOR/MONITOR'S REPORT NUMBER(S). Enter report number as assigned by the sponsoring/ monitoring agency, if available, e.g. BRL-TR-829; -215.

12. DISTRIBUTION/AVAILABILITY STATEMENT. Use agency-mandated availability statements to indicate the public availability or distribution limitations of the report. If additional limitations/ restrictions or special markings are indicated, follow agency authorization procedures, e.g. RD/FRD, PROPIN, ITAR, etc. Include copyright information.

13. SUPPLEMENTARY NOTES. Enter information not included elsewhere such as: prepared in cooperation with; translation of; report supersedes; old edition number, etc.

14. ABSTRACT. A brief (approximately 200 words) factual summary of the most significant information.

15. SUBJECT TERMS. Key words or phrases identifying major concepts in the report.

16. SECURITY CLASSIFICATION. Enter security classification in accordance with security classification regulations, e.g. U, C, S, etc. If this form contains classified information, stamp classification level on the top and bottom of this page.

17. LIMITATION OF ABSTRACT. This block must be completed to assign a distribution limitation to the abstract. Enter UU (Unclassified Unlimited) or SAR (Same as Report). An entry in this block is necessary if the abstract is to be limited.

FY2015 Final Report
AFOSR Grant – FA9550-12-1-0261
Reconfigurable Optical Directed-Logic Circuits

Jacob T. Robinson and Qianfan Xu
Rice University

1. Motivation for Directed-Logic Circuits

Directed-logic is an innovative optics-inspired paradigm to calculate Boolean functions [1]. In directed-logic architectures, all switches flip simultaneously thus switching times do not accumulate as more elements are added to a given logic circuit. This simultaneous switching stands in contrast to electronic transistor logic circuits wherein gate delays are cascaded resulting in increased latencies with increased logic elements. Thus directed-logic architectures can significantly minimize the latency required to calculate complex logic functions by taking advantage of the fast and low-loss propagation of light. For instance, directed-logic architectures could find applications in packet-switched optical interconnect networks by providing fast routing-table lookup.

2. Integrated Photonics for Directed-Logic Circuits

As a proof-of-concept demonstration we developed a 2×2-arrayed directed-logic circuit [2] based on the multi-spectral implementation as discussed in [3] which is conceptually similar to pass transistor logic in electronics [4]. One limitation of the previously demonstrated circuit is the relatively slow response time of each switch. Because these switches consisted of micro-ring resonators with embedded p-i-n junctions operating in the carrier injection mode [5] the slow switching speeds limited the circuit to low frequency operation.

With AFOSR support we have developed an improved logic circuit by employing the fast response time of the carrier depletion effect [6]. The basic building block of the logic circuit is a reconfigurable electro-optical (EO) 1 x 1 switch based on silicon micro-ring resonators. Each switch has an embedded lateral pn junction for logic input and a silicon n- doped slab micro-heater [7] for reconfiguration. This type of switch has small size[8], fast switching speed [9], low power consumption [6] and can be integrated at very large scales [10].

3. Directed-Logic Circuit Fabrication

The EO logic circuits are fabricated using the OPSIS service through a CMOS photonics foundry at the Institute of Microelectronics of Singapore. The fabrication starts on a silicon-on-insulator (SOI) wafer with 220-nm-thick top silicon and 2-μm-thick buried oxide. Rib waveguides with 500-nm width, 220-nm height and 90-nm slab thickness are used to construct the photonic circuit that only support the fundamental quasi-TE mode[2]. The switches consist of micro-ring resonators with diameters of about 35 μm

that are side-coupled to straight waveguides. A deep-UV lithography process is used to define the device pattern, which is etched into the silicon layer by inductively-coupled plasma etching. Following the etching, the p- region is doped by Boron with a dosage of 5×1012 cm-2 and ion implantation energy of 16 keV while the n- type region is doped by Phosphorus with a dosage of 3×1012 cm-2 and ion implantation energy of 45 keV . These doping regions are defined across the ring, as illustrated in the inset figure of Fig. 1(a). For both p+ and n+ doping region, the dosage and ion implantation energy are set to be 4×1015 cm-2 and 30 keV respectively. To reduce optical absorption we designed the edge of the ring waveguide to be 0.75 μm from the edge of these heavily doped regions. A 2.1-μm-thick SiO2 layer is then deposited onto the wafer using plasma-enhanced chemical vapor deposition (PECVD). Finally, vias are opened on the implanted areas, and a 2-μm-thick aluminum layer is sputtered and etched to form the electric connections. After the fabrication process, the contact pads on the chip are wire-bonded to a custom-made interface board as shown in Fig. 1(b). Each micro-heater is controlled by a power source KD3005D. The pn junctions of the switches are wire-bonded to SMA connectors with 50-Ohm terminated resistors for impedance matching.

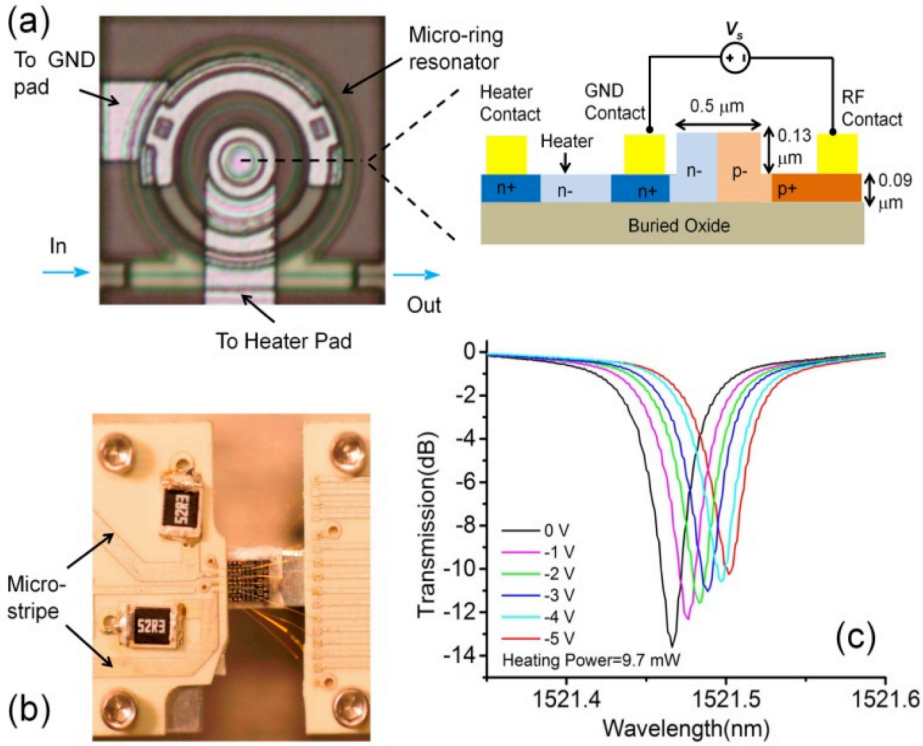

Fig. 1. (a) Optical micrograph of the electro-optic switch. The inset figure shows a cross sectional diagram of our device. Here V_s is the applied electric RF signal. The width of the waveguide is 0.5 mm and the height of waveguide is 220 nm. The thickness of the slab is 90 nm (b) The device is mounted on a stage and is wire-bonded to a printed circuit board (PCB) .There are 50-Ohm terminated resistors on PCB for impedance matching. (c) The transmission spectra of a switch at different reverse- bias voltages.

4. Directed-Logic Circuit Operation and Characterization

To characterize the resonance properties of the rings we measured the quasi-TE transmission spectra for a switch with a gap width of 350 nm using a tunable laser while the pn junction is reversed biased at a voltage ranging from 0 V~ -5 V. Sharp resonance dips can be clearly seen in Fig. 1(c). When the bias voltage is 0 V, the ring is initially quite close to the critical coupling condition in which the round trip loss in the cavity is equal to the coupling efficiency. We measure the total quality factor in this configuration to be about 32,000. Based on the plasma dispersion effect, the refractive index of silicon can be changed by injecting/removing free carriers [11]. Thus when the reversed-bias voltage is applied, the free carriers are swept out of the resonant cavity while the loss of the cavity will decrease and the refractive index will increase. Thus the resonant wavelength will be red shifted and total quality factor slightly increases to 38,000. From this data we calculate a resonance shift per unit voltage of 7.1 pm/V. In all transmission spectra, the depth of the resonance dip exceeds 10 dB, promising high extinction ratios as the ring is tuned from high to low transmission states for optical switching.

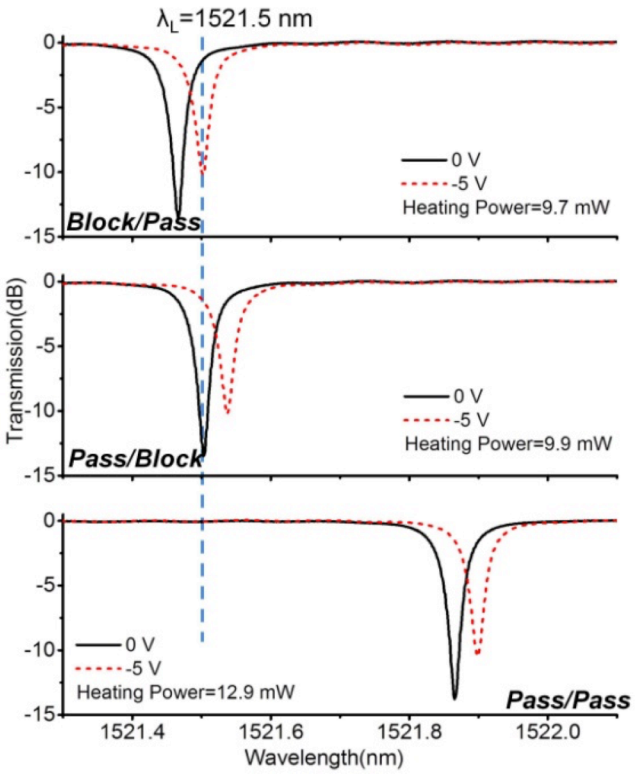

Fig. 2. (a) The transmission spectra of a switch in *block/pass* mode for light at working wavelength λ_L. The red dashed line and the black solid line are the spectra when the applied modulation signal is -5 V and 0 V, respectively. (b) The transmission spectra of a switch in *pass/block* mode. (c) The transmission spectra of a switch in *pass/pass* mode

Each switch can be reconfigured by thermal tuning to one of three operation modes, as shown in Fig. 2. At the input laser wavelength of λL = 1521.5 nm, the optical

transmission is low when voltage is reverse biased at -5 V (logic '1') and the transmission is high when the bias voltage is zero (logic '0'). So the switch works in the block/pass mode. In the block/pass mode, the optical output will be the inverse of the electronic logical input. As the working wavelength is fixed at 1521.5 nm, the operation mode can be reconfigured to be in the pass/block mode or the pass/pass mode, as shown in Fig. 2(b) and Fig. 2(c) respectively, by changing the heating power on the integrated micro-heater. In the pass/block mode, the optical logic output will match the electronic logic input while the optical logic output will always be '1' in the pass/pass mode regardless of the electronic logical input.

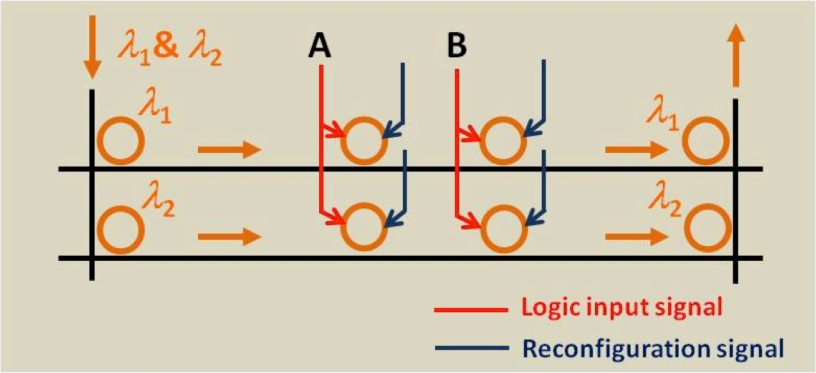

Fig. 3. Layout and the electrical actuation of the multi-spectral logic circuit.

Figure 3 shows the layout and the electrical actuation of the multi-spectral logic circuit [3] used in all of our experiments. The structure of the reconfigurable logic circuit for arbitrary two-input logic functions is illustrated in Fig. 4. The two-plus-two optical switches are connected by two optical waveguides marked as the horizontal black lines. The two vertical black lines in Fig. 4 represent the optical input and output waveguides. The electrical logic input signals (operands A and B), represented by red lines, are applied on the optical switches. Each operand controls two switches in different waveguides simultaneously. Light can pass a waveguide (corresponding to output logic '1') only when both switches are in the pass state. Thus a product function (logic AND operation) is obtained in the end of the horizontal waveguide depending on the operation mode of the two switches. For example, if the switch controlled by A is in the block/pass mode and the switch controlled by B is in the pass/block mode, the optical output carries the product AB. If the switch controlled by A is in the pass/block mode and the other switch is in the pass/pass mode, the optical output is A. This way, by reconfiguring the operation modes of the two switches in this waveguide, any product between the two operands, their inversion and '1' can be obtained at the end of each horizontal waveguide. Any two-input combinational logic function can be expressed as a sum (logic OR operation) of two products. We can perform the sum operation by incoherently adding the output optical signals from the two waveguides that calculate the two products. In our design, the micro-rings in the same horizontal waveguide are designed to have the same diameter and same resonant wavelength while rings at different horizontal waveguides have slightly different diameters and have different resonant wavelengths. For instance, the two rings in the top horizontal waveguide work at resonant wavelength λ1 while the

two rings in the bottom horizontal waveguide work at resonant wavelength λ2. Because these two waveguides operate at different wavelengths we can combine their outputs and avoid optical interference. To couple light of different wavelengths into the horizontal logic waveguides, we couple two lasers with wavelengths λ1 and λ2 into a single input waveguide (Fig. 4). We then separate these two wavelengths using passive micro-ring add/drop filters at the crossing point between the input and two logic waveguides (left side of Fig. 4). After light passes through the horizontal switch array, the light is redirected to an output (vertical) waveguide if the micro-ring add/drop filter at the crossing point is on resonance (right side of horizontal waveguides and represented by the orange circles). Light will not be collected when the output micro-ring resonator is tuned away from the laser wavelength (represented by the green dashed circles). In our circuit, we can thermally tune the resonance of the output micro-ring add/drop filter [2].

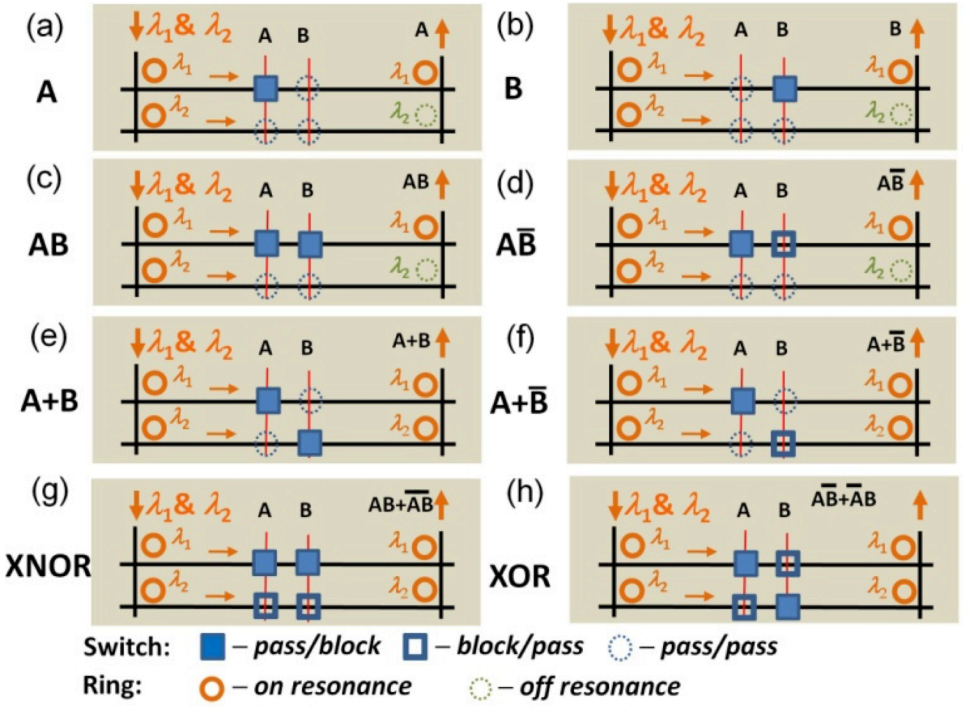

Fig. 4. Circuit diagrams of the electro-optical directed-logic circuits for different two-input logic functions.

Light at the end of the output optical waveguide is sent to the broadband photodetector of the high-speed oscilloscope, which absorbs photons from all source wavelengths and creates a photocurrent proportional to the optical power from all horizontal waveguides. This summation represents a logical OR function by defining '1' as the power collected if any one of the horizontal waveguides has a high-level output.

To combine the light from both horizontal logic waveguides into the vertical output waveguide we use add/drop micro-ring filters at the waveguide crossing points. These micro-ring resonators are critically coupled and we can adjust the add/drop wavelength using integrated micro-heaters. Once the add/drop filter is set to the appropriate wavelength, there is no need for fast switching thus we have not embedded any pn junctions into these rings. The coupling gap of the add/drop ring is set to be 200 nm to enlarge the coupling efficiency. As the intrinsic loss of the ring cavity is negligible

compared with the coupling efficiency, the add/drop ring is still under the critical coupling condition with an extinction ratio larger than 20 dB. This high extinction ratio promises high power--drop efficiency at the resonant state [12]. The large coupling efficiency can also broaden the coupling bandwidth and reduce the thermal instability in the ring cavity. At the crossing points between the waveguides, the width of the waveguide is increased to 1 μm in order to reduce the optical loss [2]. We couple light into the waveguides using tapered-lens fibers and on-chip Si inverse tapers with 180-nm-wide tips which are integrated for input and output terminals of the waveguides. The coupling loss is about 5 dB per facet.

5. Demonstration of Optical Directed-Logic at 3 GHz

We have implemented all the sixteen possible two-input logic functions by thermally reconfiguring the operation modes of the switches and by tuning the output add/drop micro-ring resonators. We have included in Fig. 4 the results of eight representative logic functions. The two laser wavelengths are fixed at 1514 nm and 1521.5 nm in all the demonstrations. The two logic signals are fixed at a bit-rate of 2.95 Gb/s with voltage ranges from -4.5 V (logic '1') to 0 V (logic '0'). To create two logic signals from one 2.95 Gb/s source we amplify the RF signal from pulse pattern generator and then split the amplified signal into two channels with independent tunable delays. Logic input 'A' is driven by one of the two RF signals while logic input 'B' is driven by the other RF signal that is delayed by several bits. Here 4.5 Vpp is the maximum peak to peak voltage after power splitting. The consumed RF power for each optical switch is about 300fJ/bit or 0.9 mW if we take the capacitance of ring resonator to be 58 fF [6]. The device 3 dB modulation bandwidth is calculated to be 6 GHz [6], limited by the photon lifetime in the cavity. The average heating power used in the demonstration is about 4 mW for the optical switch and 43 mW for the add/drop ring . Here the heating power difference is due to resonance misalignment between optical switches and add/drop rings from fabrication process. The thermo-optic reconfiguration time is measured to be <40 μs. Since we use an n-doped silicon slab micro-heater, the heating energy can easily dissipate through the slab region. Thus, the heating efficiency here is lower than in our previous work where we use TiN as the micro-heater [2]. For each optical switch, the group delay is calculated to be about 300 ps when the micro-ring is on resonance (light is blocked) while it is about 0.25 ps when the micro-ring is off resonance. The output powers of the two lasers are both set to be 3 dBm. They are combined with a 50/50 fiber coupler and then coupled into the circuit.

Fig. 4(a)-(h) shows the circuit diagrams with the operation modes of the switches and the output rings when each logic function is performed. The waveforms of the output optical signal are shown in Fig. 5(a)-(h). In (a) and (b), the output logic signals are equivalent to the input A and B, respectively. In (a)-(d), the logic function has only one product thus only light from the top waveguide is coupled to the output waveguide. In (e) and (f), the two high output powers correspond to the case when one waveguide passes light and when both waveguides pass light, respectively. Both of these power levels are judged as logic '1'. In (a)-(h), the output power oscillates increasing the variability in the logical '1' power level. We note that in this configuration optical power oscillations

occur at the transition of logic input signals from '0' to '1' or from '1' to '0'. These power oscillations should not come from the beat between trapped light in the high-Q resonator and transmitted light as beat's decaying time constant is determined by the photon lifetime (~25 ps) which is much smaller than the decaying time constant of the power oscillation (~160 ps) here [13]. Thus these power oscillations are the result of an oscillating density of electrons and holes in the cavity as this carrier density evolves toward steady state levels. These oscillations match the transient response of an LC circuit where the inductor (L) is created from the bonding wire [14] and the capacitor (C) results from the reverse- biased pn junction [6]. In this circuit, this electron oscillation frequency is measured to be about 6 GHz which is the main factor limiting the operating speed of our logic circuit. In (c)-(h), there are occasional positive spikes between two consecutive '0's that occur when one switch turns off while the other switch turns on. The height of this power spike depends on the timing of the rising and falling edges of the two switches. The spikes do not affect correct decoding of the bits because these artifacts occur in the bit transition regions.

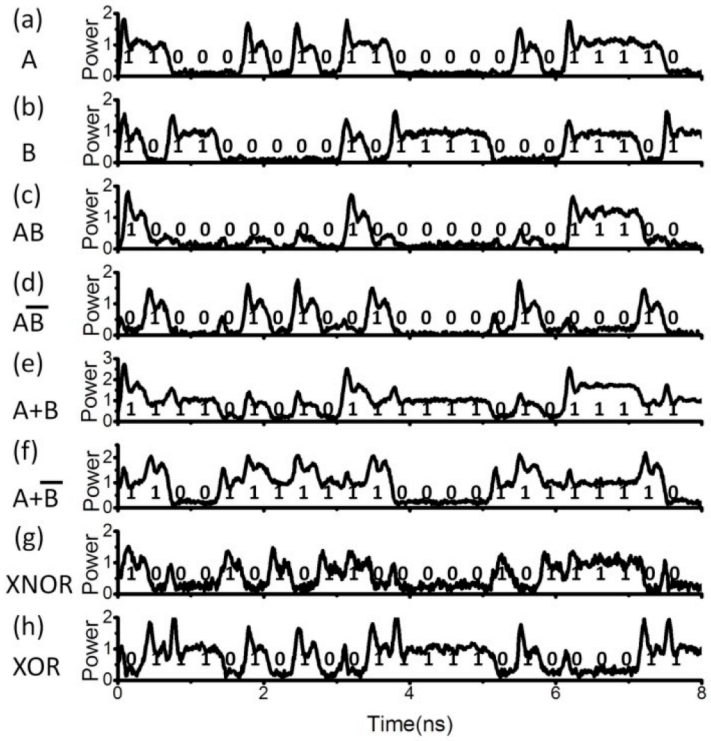

Fig. 5 . Waveforms of the output optical signal from the two-input directed-logic circuits shown in Fig. 4. The two input electrical control signals are non-return-to-zero (NRZ) 2^7-1 pseudo-random bit sequence signals at 2.95 GHz. They are both set to be 4.5 V_{pp} from -4.5 V to 0V.

7. Visible wavelength photonics

To expand the possible applications of our technology we have begun investigating photonic elements that could route and manipulate light at visible wavelengths. For example, displays, cameras and fluorescence all rely on illuminating or collecting visible

light (wavelengths between the 400-700 nm). Thus waveguides, resonant cavities, and modulators that function within this wavelength range would open up new application areas. To reach this goal we have begun fabricating photonic devices in Aluminum Nitride (AlN_4). This material is ideal for high-speed visible light photonics because it has a high-index of refraction (ordinary refractive index n_o=2.17 at 488 nm), large electro-optic coefficient (r_{33}, r_{13}~1 pm/V), and can be fabricated into low loss waveguides [15]. Unlike silicon, AlN4 has an electro-optic response due to the c-axis aligned non-centrosymmetric crystal orientation that results from sputter deposition. As a result we can tune the refractive index by applying an electric field without relying on the plasma dispersion effect (and the associated electron-hole recombination rates that ultimately limit the modulation speed). We expect that the electro-optic effect in AlN4 will allow us to operate devices at speeds greater than 12.5 GHz (as has been reported for AlN4 modulators).

To fabricate photonic devices in AlN, AlN thin films are deposited onto the 3-inch glass wafer using AJA UHV six-source sputtering system. The aluminum target with purity 99.999% are sputtered in a nitrogen and argon gas mixture with deposition pressure of 2 mTorr. The flow rates of nitrogen and argon are optimized to be around 13.3 and 20 sccm, respectively. The sputtering DC power is 250 W and RF power is 50 W. The photonic circuits are patterned using electron beam lithography on JEOL JBX 5500FS eBeam writer. Using the inductively coupled plasma (ICP) reactive ion etching, the patterns are transferred to the AlN film in Cl2/BCl3/Ar flow at the rate of 25/9/6 sccm, respectively. Under pressure of 5 mTorr, the film is etching at the RF power of 70 W and ICP power of 360 W. In this case the etching rate for AlN film and HSQ resist are 176 nm/min and 40 nm/min and the etching selectivity is about 4.4:1. Using atomic force microscope (AFM), the AlN film surface roughness is measured to be 0.96 nm rms before etching and 1.03 nm rms after etching, which is much less than the optical wavelength 488 nm.

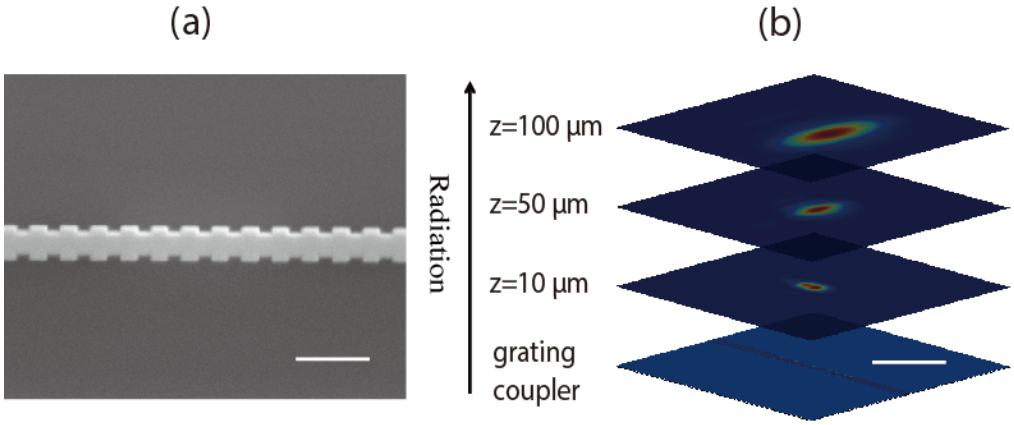

Fig. 6. (a) SEM image of an AlN grating coupler, scale bar is 500 nm. (b) FDTD simulation of the vertical radiation pattern, scale bar is 20 µm.

As a proof-of-principle we have fabricated grating couplers to radiate light out of the plane of the chip. Devices like these will allow us to visualize the output of a logic circuit and could be used as a source for a display or fluorescence illumination. Fig. 6 shows (a)

a SEM image of the grating coupler and (b) an FDTD simulation showing the expected radiation pattern. The period of the grating is 320 nm and duty cycle is 0.5. The width of narrow and wide section are 200 and 300 nm, respectively.

To test our AlN4 waveguides and resonant cavities have implemented a wet chemical etch to produce an adiabatic taper that has been shown to efficiently couple into waveguides [16]. Tapered optical fibre tips were fabricated by etching the tip in 48% aqueous hydrofluoric acid (HF) with an organic protective layer of 1-bromodecane. Prior to etching, the fiber end to be etched was soaked in acetone for 8 minutes to remove the acrylate jacket. The speed, direction and etching time of the fiber motion were controlled by computer. The tip was made by moving down at 90 μm/min for 45 mins. After the tip was etched, the fiber was pulled out of the solution at 1620 μm/min for 5 minutes. The fibre tips were then rinsed with deionized water and ethanol repeatedly. The tip diameter, cone angle and total taper length can be adjusted by tuning the moving speed and etching time. Fig. 7 shows an SEM image of a typical adiabatic fiber taper with 129 nm tip diameter, 3.6^{o} cone angle and 1819 μm total taper length.

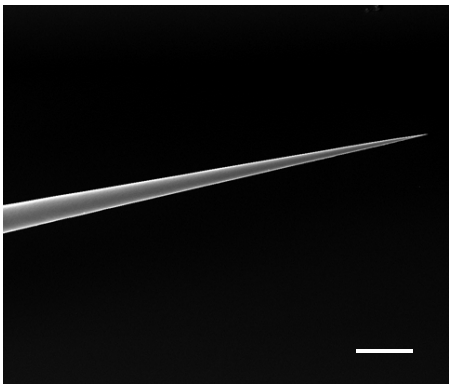

Fig. 7. SEM image of a fibre taper with cylindrical tip diameter of 129 nm, scale bar is 50 μm. The cone angle is 3.6^{o} and the total taper length is 1819 μm.

Based on this approach we expect to demonstrate a series of new visible light photonic technologies similar to what we have developed in silicon.

6. Summary

In conclusion, we have demonstrated an improved electro-optic directed-logic circuit with increased operational speed by using integrated optical switches based on the carrier depletion effect. Our proof-of-concept implementation shows that a small-scale multi-spectral circuit can be reconfigured to perform arbitrary two-input combinational logic functions. The demonstrated speed of ~3 Gb/s is currently limited by the inductance of the wire-bonds and capacitance of the pn junction. We expect higher speed operation is possible by improving the probing method or reducing the inductance of the bonding wire by shortening the wire length.

Going forward we see opportunities for new applications by using AlN as a core material. This new material system will both allow us to operate at higher speeds and access new applications that may be specific to visible light (e.g. microscopy, displays, cameras). We have begun testing our fabrication and testing procedures and expect that this work will lead to new visible light photonic technologies in the years to come.

7. References

1. J. Hardy, and J. Shamir, Opt Express 15, 150-165 (2007).
2. C. Qiu, X. Ye, R. Soref, L. Yang, and Q. F. Xu, Opt Lett 37, 3942-3944 (2012).
3. Q. Xu, and R. Soref, Opt Express 19, 5244-5259 (2011).
4. D. Markovic, B. Nikolic, and V. G. Oklobdzija,Microelectr J 31, 991-998 (2000).
5. Q. Xu, B. Schmidt, S. Pradhan, and M. Lipson, Nature 435, 325-327 (2005).
6. P. Dong, S. R. Liao, D. Z. Feng, H. Liang, D. W. Zheng, R. Shafiiha, C. C. Kung, W. Qian, G. L. Li, X. Z. Zheng, A. V. Krishnamoorthy, and M. Asghari, Opt Express 17, 22484-22490 (2009).
7. K. Xiong, X. Xiao, X. Y. Li, Y. T. Hu, Z. Y. Li, T. Chu, Y. D. Yu, and J. Z. Yu, Opt Commun 285, 4368-4371 (2012).
8. Q. Xu, D. Fattal, and R. G. Beausoleil, Opt Express 16, 4309-4315 (2008).
9. F. Y. Gardes, A. Brimont, P. Sanchis, G. Rasigade, D. Marris-Morini, L. O'Faolain, F. Dong, J. M. Fedeli, P. Dumon, L. Vivien, T. F. Krauss, G. T. Reed, and J. Marti, Opt Express 17, 21986-21991 (2009).
10. A. Biberman, and K. Bergman, Rep Prog Phys 75 (2012).
11. R. A. Soref, and B. R. Bennett, Ieee J Quantum Elect 23, 123-129 (1987).
12. F. Monifi, J. Friedlein, S. K. Ozdemir, and L. Yang, J Lightwave Technol 30, 3306-3315 (2012).
13. Q. F. Xu, B. Schmidt, J. Shakya, and M. Lipson,Opt Express 14, 9430-9435 (2006).
14. Y. Akazawa, N. Ishihara, T. Wakimoto, K. Kawarada, and S. Konaka, Ieee J Solid-St Circ 21, 417-423 (1986).
15. X. Chi, W. H. P. Pernice, and H. X. Tang, Nano Lett 12, 3562-3568 (2012).
16. L. H. Haber, R. D. Schaller, J. C. Johnson, and R. J. Saykally. Journal of Microscopy 214, 27-35 (2004).

1.

1. Report Type

Final Report

Primary Contact E-mail

Contact email if there is a problem with the report.

jacob.t.robinson@rice.edu

Primary Contact Phone Number

Contact phone number if there is a problem with the report

713-348-2933

Organization / Institution name

Rice University

Grant/Contract Title

The full title of the funded effort.

Reconfigurable Optical Directed-Logic Circuits

Grant/Contract Number

AFOSR assigned control number. It must begin with "FA9550" or "F49620" or "FA2386".

FA9550-12-1-0261

Principal Investigator Name

The full name of the principal investigator on the grant or contract.

Jacob Robinson

Program Manager

The AFOSR Program Manager currently assigned to the award

Pomrenke Gernot

Reporting Period Start Date

01/02/2012

Reporting Period End Date

06/14/2015

Abstract

Directed logic (DL) is an innovative logic paradigm that minimizes the latency in calculating a complicated logic function by taking advantage of the fast and low-loss propagation of light. DL can enhance the performance of digital systems for real-time applications that are especially important for Air Force missions, such as video analysis, object recognition, visualization and battle management. DL can also provide very fast network routing functions, which enable highly efficient packet-switched interconnection networks for high-performance computing.

A DL circuit is formed by a network of optical switches controlled by the input logic signals. The optical wave travelling in the switch network calculates a logic function of the control signals. While it takes time for each switch to respond to a change in its control signal, all the switches operate simultaneously, and their switching delays do not accumulate. This is in contrast to conventional logic circuits where gate delays are cascaded, resulting in a large latency in a complex logic circuit.

In this project, we will develop a new cellular DL architecture based on large-scale integrated silicon photonic circuits. The circuit is formed by a uniform two-dimensional array of reconfigurable optical switches based on silicon micro-resonators. The switches should have small size, fast switching speed, high extinction ratio, low insertion loss and ultra-low power consumption. We will demonstrate in this project a switch based on coupled dual-ring resonators that satisfies all those requirements with significant

improvement over state of the art.

Distribution Statement

This is block 12 on the SF298 form.

Distribution A - Approved for Public Release

Explanation for Distribution Statement

If this is not approved for public release, please provide a short explanation. E.g., contains proprietary information.

SF298 Form

Please attach your SF298 form. A blank SF298 can be found here. Please do not password protect or secure the PDF The maximum file size for an SF298 is 50MB.

SF298_Robinson.pdf

Upload the Report Document. File must be a PDF. Please do not password protect or secure the PDF . The maximum file size for the Report Document is 50MB.

AFOSR_Final Report.pdf

Upload a Report Document, if any. The maximum file size for the Report Document is 50MB.

Archival Publications (published) during reporting period:

Changes in research objectives (if any):

Change in AFOSR Program Manager, if any:

Extensions granted or milestones slipped, if any:

AFOSR LRIR Number

LRIR Title

Reporting Period

Laboratory Task Manager

Program Officer

Research Objectives

Technical Summary

Funding Summary by Cost Category (by FY, $K)

	Starting FY	FY+1	FY+2
Salary			
Equipment/Facilities			
Supplies			
Total			

Report Document

Report Document - Text Analysis

Report Document - Text Analysis

Appendix Documents

2. Thank You

E-mail user

Nov 10, 2015 13:08:17 Success: Email Sent to: jacob.t.robinson@rice.edu